C. R. Mecanique 343 (2015) 301–306

Contents lists available at ScienceDirect

Comptes Rendus Mecanique

www.sciencedirect.com

Catching the time evolution of microstructure morphology from dynamic covariograms

Évolution temporelle de la morphologie de la microstructure à partir d'un covariogramme dynamiques

Nait-Ali Azdine *, Kane-diallo Ousseynou, Castagnet Sylvie

ISAE–ENSMA, Institut Pprime, UPR CNRS 3346, département "Physique et mécanique des matériaux", ENSMA, Téléport 2, 1, avenue Clément-Ader, BP 40109, 86961 Futuroscope Chasseneuil-du-Poitou cedex, France

ARTICLE INFO

Article history:
Received 19 January 2015
Accepted 25 February 2015
Available online 14 March 2015

Keywords:
Morphological analysis
Dynamic covariogram
Random medium
Damage kinetic
Ergodic theory
Micromechanical modelling

Mots-clés :
Analyse morphologique
Covariogramme dynamique
Milieu aléatoire
Cinétique d'endommagement
Théorie ergodique
Micro-mécanique

ABSTRACT

In micromechanical modelling, covariograms are often used as a statistical analysis to estimate the features or morphological Representative Elementary Volumes (REV), from representative pictures of the initial microstructure (i.e. static covariogram). The aim of this article is to present an extension of the method to the time evolution of the microstructure, through the idea of dynamic covariogram built up of successive pictures of the microstructure along time. The possible enhanced evolution of covariogram parameters is analyzed first from a general point of view. It is then illustrated on the cavitation damage occurring during decompression in rubbers exposed to diffusing gas.

RÉSUMÉ

En micromécanique, la construction de covariogramme est utilisée pour renseigner la notion de volume élémentaire représentatif morphologique, à partir d'images représentatives de la microstructure initiale. L'objet de cet article est de présenter une extension de cette notion à l'évolution temporelle de la microstructure au cours du temps, via la notion de covariogramme dynamique, issue d'images successives de la microstructure au cours du temps. L'évolution possible des différents paramètres du covariogramme est analysée de manière standard, puis illustrée à partir de l'endommagement par cavitation observé dans les élastomères sous décompression après exposition à un gaz diffusant.

1. Introduction

In micro-mechanics, a rigorous definition of the Representative Elementary Volume (REV) is needed, either for analytical modeling or for full-field numerical simulations. REV implies to be representative of both the microstructure morphology and the mechanical properties. Only the morphological aspect is addressed here. Microstructure within the morphological

* Corresponding author.
E-mail addresses: azdine.nait-ali@ensma.fr (N.-A. Azdine), ousseynou.kane-diallo@ensma.fr (K.-d. Ousseynou), sylvie.castagnet@ensma.fr (C. Sylvie).

http://dx.doi.org/10.1016/j.crme.2015.02.005
1631-0721/

REV can be more or less finely defined. Basic descriptions are often based on the volume fraction of components only, but more sophisticated descriptors can be used too, for instance the size distribution of inclusions or porosity, or the shape factor distribution in case of anisotropic particles. The REV description can be based on stochastic considerations. When inclusions are stochastically distributed, the REV is called DREV, standing for Deterministic Representative Elementary Volume. A fine morphological description of the REV can be obtained using image analysis through covariogram [4–6]. Many different data can be estimated from this statistical analysis method, among which the size of the REV, the number of included phases, the isotropy or the ergodicity of the distribution of inclusions. Such a concept has been widely used so far, almost systematically to static cases, i.e. to images of the initial microstructure. The covariogram analysis is used to identify parameters of the schematized microstructure or generate numerical models, in analytical or full-field numerical models respectively. Microstructure morphology is not updated during the simulation. The aim of this paper is to extend this approach to so-called dynamic cases, i.e. situations for which the microstructure evolves with time, like during damage processes for instance. Indeed, the REV changes occurring during the damage process can be tracked through the evolution of covariograms parameters deduced from successive snapshots of the microstructure. In the following, only heterogeneous materials made of two phases will be considered. The article is divided into two parts. The first part briefly describes useful parameters displayed by covariograms. The second part is dedicated to the mechanical interpretation of these parameter evolutions. As a first example about material cracking, it is explained how privileged cracking directions and/or evolution of these directions can be pointed out from REV evolution. A second example deals with the ability of covariograms to highlight damage evolution during cavitation damage occurring during transient diffusion loadings.

2. Covariogram parameters obtained from a single picture of the initial microstructure (static case)

This first section briefly reminds the statistical framework of covariogram analysis and introduces relevant parameters that can be deduced for microstructure description. The same parameters will be further considered in the dynamic case, to highlight the physical interpretation of complex transient phenomena.

No difference is made between R^3 and the three-dimensional Euclidean physical space equipped with an orthogonal basis denoted by (e_1, e_2, e_3). Let us consider the set $\Omega \in R^3$ and $X := \cup_{i\in\mathbb{N}} X_i \subset \Omega$ with X_i connex family set. For every $z \in \mathbf{Z}^2$, the operator $\tau_z : \Omega \to \Omega$ by $\tau_{-z}X := X + z$ is defined. Vector z corresponds to a direction of study. The probabilistic set X is equipped with the trace σ-algebra A of standard product σ-algebra on $\mathbb{R}^3$. Then, the probability space $(\Omega, A, \mathbf{P})$, with P a probability measure, can be defined. The covariogram describes the probability that both events X and $\tau_{-z}X := X + z$ occur simultaneously. In direction z, Eq. (1), the covariogram function is defined by:

$$\begin{aligned} &C : \mathbb{R}^3 \to \mathbb{R} \\ &z \to C(z) \\ &C(z) = \mathbf{P}\{x \in X \cap \tau_{-z}X\} \end{aligned} \tag{1}$$

Covariogram can be viewed as a concept close to pair-correlation functions. Such a function corresponds to the probability to intercept other particles at a distance h from a reference particle. It is obtained by growing a sphere of radius h from this reference particle. Firstly, pair-correlation function is not calculated for a given direction and is thus unable to quantify anisotropy. Secondly, unlike covariogram, pair-correlation function provides representative information if it is independent of the choice of the reference particle, i.e. in case of a homogeneous distribution. Covariogram is thus a more general tool for quantification of microstructure morphology.

It can be pointed out easily from this definition that if the material is periodic, then the function $C(\cdot)$ is periodic too. When applied to image analysis, if noting I the characteristic function of pixel x (i.e. $I(x) = 1$ if $x \in X$ and 0 otherwise), the definition of the covariogram becomes (Eq. (2)):

$$C(z) = \int_{\Omega} I(x)\cdot I(x+z)\,\mathrm{d}x \tag{2}$$

In this work, the calculation of covariograms is based on the Fast Fourier Transform (FFT). Therefore, it allows us to work in a frequency space, and therefore, the medium is considered infinite.

For easier reading, the evolution of the covariogram according to any direction z is noted $C_z(\cdot)$. For a heterogeneous bi-phasic medium like that depicted in Fig. 1—left, the domain X can be associated with one phase, e.g., with inclusions. It is then possible to get statistical data related to this phase. For instance, the right part of Fig. 1 displays covariograms along the horizontal (X) and vertical (Y) directions. Curve shapes are classical for such a microstructure.

More particular properties of the covariogram are listed below.

$(\mathcal{P}_1)$ – It can be noticed first that the volume fraction of phase X is directly given by the covariogram for $h = 0$:

$$C_z(0) = \mathbf{P}\{x \in X\} := f_X$$

with f_X the volume fraction of X in the medium Ω.

$(\mathcal{P}_2)$ – If an horizontal asymptote line exists when h tends to the higher values, moreover with a value $C(z) = f_X^2$, then the probability distribution is ergodic, meaning that the distribution is homogeneous. The occurrence probability is the

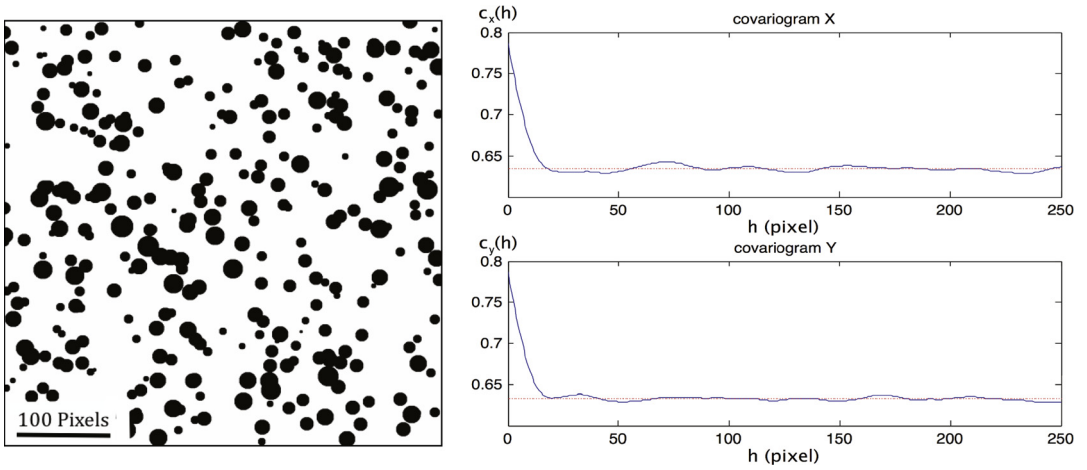

Fig. 1. (Color online.) Example of covariogram for a heterogeneous media.

same at any point of the volume. Ergodicity property is essential, for example, to build up a deterministic micromechanical modeling of a medium containing randomly distributed inclusions [7]. In this case, a stationary condition can be expressed by:

$$\forall z \in Z^2, \quad \tau_z \# \mathbf{P} = \mathbf{P} \tag{3}$$

where $\tau_z \# \mathbf{P}$ denotes the image probability of $\mathbf{P}$ by τ_z. Moreover, for any set X of A, an asymptotic mixing property [7] can be written:

$$\lim |z| \to +\infty \mathbf{P}(\tau_z X \cap X) = \mathbf{P}(\tau_\infty X)\mathbf{P}(X) = \mathbf{P}(X)\mathbf{P}(X) = C_z(\infty) = f_X^2 \tag{4}$$

The asymptotic mixing property is a sufficient condition to ensure ergodicity of probabilistic space $(X, A, \mathbf{P}, \tau_z)$. The asymptote can be different from f_X^2, meaning that the distribution is not statistically homogeneous.

$(\mathcal{P}_3)$ – If the horizontal asymptote value is the same for all directions, the microstructure is isotropic at the macroscopic scale. But values can be different depending on the direction. In this case, the material is anisotropic.

$(\mathcal{P}_4)$ – The first intersection between $C_z(h)$ and the asymptote corresponds to the correlation length in the z direction, noted $Dc(z)$. It is also called Integral Range by some authors [6]. It is defined by:

$$Dc(z) := \min_h \{Cz(h) - f_X^2 = 0\} \tag{5}$$

This distance corresponds to the maximal distance of statistical influence of the inclusion phase X. It provides information about the minimal size of the domain over which the volume is statistically representative. Beyond this distance, additional statistical information is negligible. Thus, the size of the DREV in this direction (z) can be assimilated to twice $Dc(z)$. This value is a characteristic scale of a material, used to approximate the size of DREV along direction z. If the heterogeneous medium contains clusters of inclusions, $Dc(\cdot)$ provides an estimate of the "statistical average" size of the cluster in each direction. If $Dc(\cdot)$ is constant regardless of the direction, the material is isotropic at this scale [6]. When addressing material cracking, the favorite crack orientation can be given by the maximal value of $Dc(\cdot)$ over all the possible directions z, as expressed by Eq. (6).

$$O_m := \max_z Dc(z) \tag{6}$$

$(\mathcal{P}_5)$ – The second intersection between $C_z(h)$ and the asymptote corresponds to an outdistance of repulsion in the z direction, noted $Rep(z)$. It corresponds to the statistical average distance between two inclusions, so between two subdomains of X. In clustering situations, $Rep(\cdot)$ gives an estimate of the "statistical average" distance between two clusters in each direction.

$(\mathcal{P}_6)$ – The existence of two scales (i.e. due to clusters of inclusions with two different inclusion sizes, as illustrated in Fig. 2, left) is characterized by an inflection on the covariogram before intercepting the asymptote.

Then, the correlation length $Dc(z)$ increases. The outdistance of repulsion $Rep(z)$ decreases, but slightly.

All these properties make it possible to give a morphological description and thus allow us to validate the relevance of the numerical material [7]. They can be used to adapt along the time the REV size over which numerical calculations are performed.

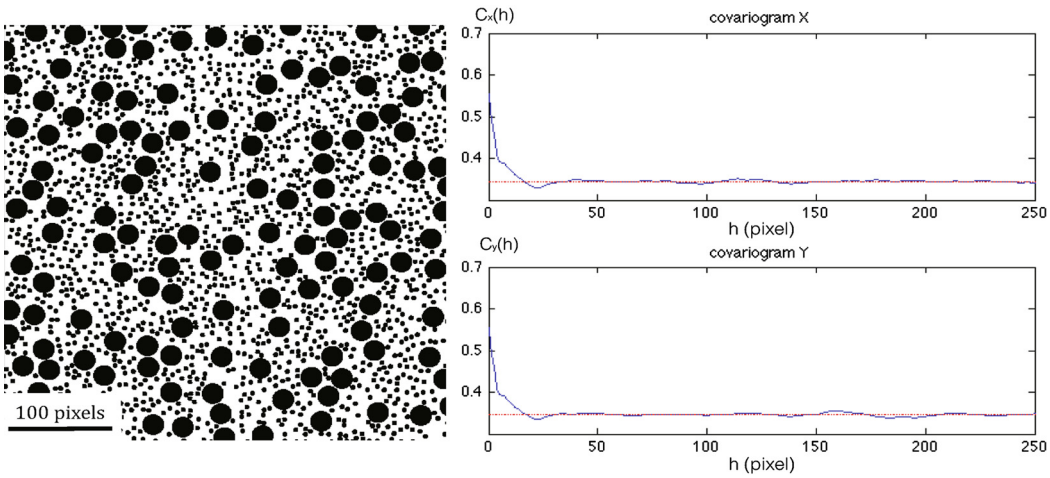

Fig. 2. (Color online.) Example of covariogram for a heterogeneous medium with the size of two inclusions (covariogram in blue and asymptot in red).

3. Dynamic case: evolution of covariograms issued from successive pictures of the evolving microstructure

This section discusses now how some time evolutions of these parameters can highlight complex mechanical phenomena like damage. It will be illustrated from the kinetics of a cavitation process in the next section. At a given time t, the covariogram analysis depicted in Section 3 can be applied to the current microstructure picture. The set of parameters listed in the previous section can be estimated at any selected time t. Current values of parameters $Dc(\cdot)$ and $Rep(\cdot)$ are noted $Dc(\cdot, t)$ and $Rep(\cdot, t)$, respectively.

($\mathcal{P}_1$) – The volume fraction corresponding to the initial value $Cz(0)$ can vary with time. This may occur for voiding, cracking, or phase transformation processes.

($\mathcal{P}_2$) – Ergodicity is bound to be established in the initial microstructure, but broken due to further time evolutions of the microstructure. It is of huge importance to detect this way the application limit of deterministic micromechanical modeling.

($\mathcal{P}_3$) – In the same way, an initially isotropic microstructure becoming anisotropic can be detected from the asymptotic values of the covariogram in different directions.

($\mathcal{P}_4$) – It is clear from Eq. (2) that the variation of the correlation length $Dc(z, t)$ with time is due to a variation of the volume fraction. It may depend on the number and/or the size and/or the shape of inclusions. In order to simplify, scenarios involving evolutions of one of these three parameters only are discussed now. In the example of Section 4, spherical cavities will be considered so that only the number and/or size are changing with time. The variation of $Dc(\cdot, \cdot)$ may also show a favorite crack orientation along the time of study. More generally we could know over time and the scale of microstructure, so the material is always isotropic comparing $Dc(z, \cdot)$ in each direction and at each time step. This information is important for the case of a numerical simulation where one has to be in cases where the model adjusts.

Let us consider first isotropic inclusions. If the number of these inclusions stays constant, an increase in $Dc(z, t)$ with time corresponds to their growth (see properties (1) and (2)). If the inclusion size is constant with time, a decrease of $Dc(z, \cdot)$ means that new cavities appear. If the number of inclusions increases, a sharp increase of $Dc(z, \cdot)$ corresponds to the onset of a second scale, i.e. new cavities appear around the already existing ones. This phenomenon can be confirmed by observing the onset of an inflexion of the $C_z(\cdot, t)$ curve just before intercepting the asymptote. Obviously, if the morphology of inclusion changes along direction z, then $Dc(z, \cdot)$ will also change and consequently influence isotropy.

($\mathcal{P}_5$) – The outdistance of repulsion $Rep(\cdot, t)$ evolves inversely to $Dc(\cdot, t)$ and proportionally to the Dc volume fraction. At constant volume fraction, it makes sense when the inclusions are growing or become larger than their respective distance decreases.

($\mathcal{P}_6$) – The equality between $AsympX$ and $AsympY$ corresponds to an isotropic distribution of the microstructure and therefore to an isotropic material. This must be considered in dynamic macroscopic modeling for numerical approach or just to validate the numerical model.

4. Example of the dynamic case: cavitation in a gas-saturated rubber upon decompression

The following section aims at illustrating some of the above-depicted features, based on the cavitation damage occurring in rubbers when decompressed after gas exposure and sorption of the gas into the rubber. Since defects are spherical cavities, some anisotropy effects will not be illustrated. When rubbers are exposed to pressurized gas for a long time, gases penetrate into the polymer until reaching a thermodynamic equilibrium state of saturation. When pressure suddenly decreases, the gas trapped within the polymer tends to expand and diffuse out of the material. If diffusion is not fast enough

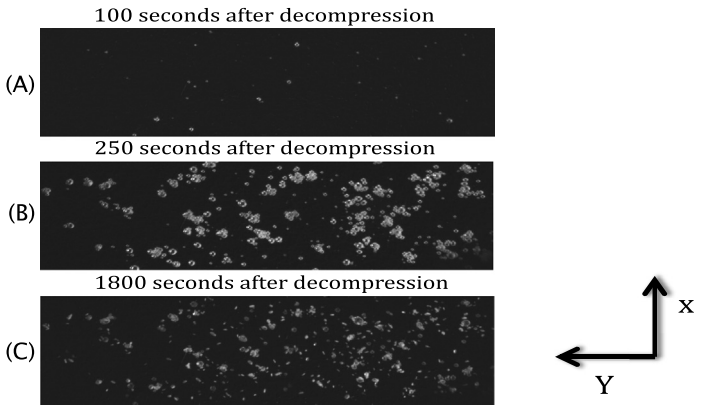

Fig. 3. Optical images of cavity fields observed (A), (B) and (C) in a transparent EPDM exposed to hydrogen at 9 MPa for 1 h and decompressed at 2.5 MPa/min at three different times.

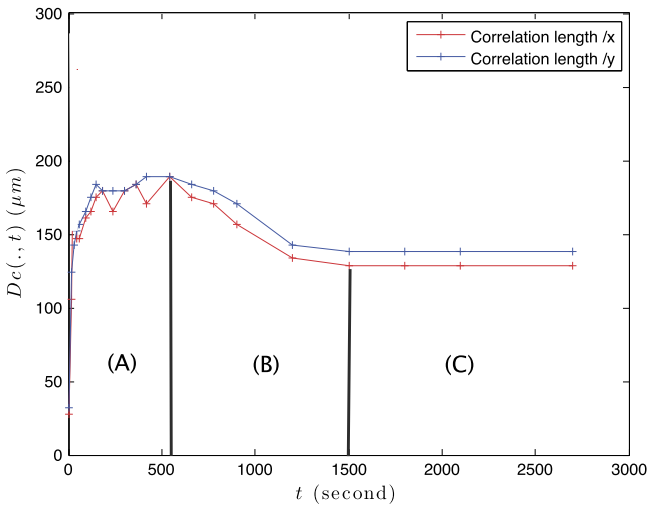

Fig. 4. (Color online.) Evolution of the correlation distance: (A) nucleation and growth of the cavities; (B) decreasing, disappearance of the second level; (C) residual damage.

compared to the decompression rate, expansion of the gas occurs within the polymer, enhancing diffuse or localized damage by cavitation, multiple cracking or even foaming [1]. This phenomenon, often referred to as "explosive decompression failure", has been evidenced for polymers exposed to various gases (H_2, CO_2, H_2S, CH_4) [3].

As illustrated in Fig. 3 in an EPDM exposed to hydrogen under 9 MPa and decompressed at 2.5 MPa/min, a first step corresponds to more or less delayed cavity nucleation (step A). Then the first cavities start to decrease, while the last ones still inflate (step B). Finally, all remaining cavities decrease (step C). Only a very few works reported time-resolved data about cavities nucleation and growth, especially during decompression [7,8]. Damage morphology and kinetics were shown to depend on the decompression conditions: decompression rate and saturation pressure. Several populations of cavities were observed sometimes, i.e. primary cavities surrounded by smaller satellite ones [2].

Subsequent differences and time evolutions of cavity field statistics can be captured by covariograms issued from successive pictures.

Fig. 4 compares the time evolution of the correlation length *Dc* along the directions *X* and *Y* of images in Fig. 3. As underlined in the previous section, both the number and size of cavities are bound to affect *Dc*. An increase in *Dc* means that at least the number of the size or cavities increases too. Fig. 3 displays one more data, i.e. the evolution of the number of cavities with time. It helps to interpret the three successive steps A, B and C, as nucleation and growth (A), decrease and disappearance (B) and persisting damage (C) respectively. Obviously, these interpretations are also due to the number of cavities according to time.

At any time, correlation lengths along *X* and *Y* are almost identical; the difference never exceeds 7%. Values could be different, e.g., in case of clustering or cracking in a privileged direction. However, the correlation length evolves with time for a given direction. It means that analytical modeling or numerical computations should take into account an evolutive DREV with time or consider an upper bound over the time range.

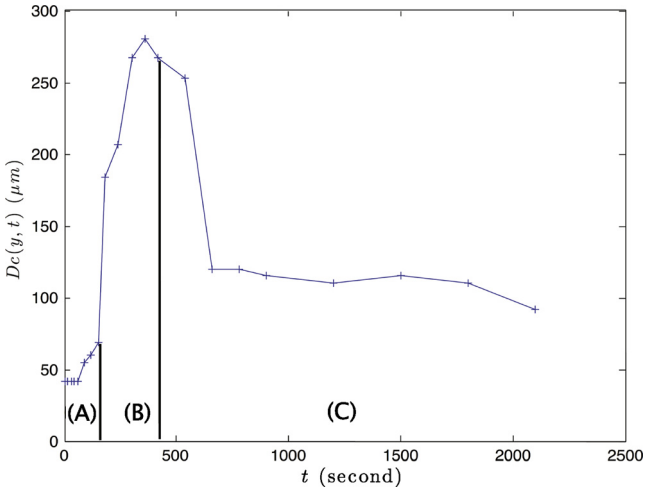

Fig. 5. Evolution of the correlation distance: (A) nucleation and growth of the cavities; (B) growth of cavities nucleation and cluster training of cavities (double scale); (C) decreasing, disappearance of the second-level and residual damage.

For higher decompression rates, the damage kinetics is different. As shown in Fig. 5, three steps can be distinguished: the first step (A) corresponds to the nucleation and growth of the first cavities, the second stage (B) corresponds to the onset of additional cavities around the existing ones, and finally during step (C) cavities decrease until they stabilize, leading to a residual damage. More precisely, between stages A and B the huge increase of *Dc* can arise from the onset of a cluster of inclusions. Indeed, the presence of a cluster increases the statistical length of influence and thus *Dc*. And between stages B and C, this cluster disappears.

All these features, supported by covariogram analysis, could not be pointed out, and even less quantified, through observation with the naked eye.

5. Conclusion and future prospects

The covariogram method, so far used for morphological analysis in static or stationary cases, has been extended here to a time-dependent framework, i.e. applied to a set of time-resolved pictures of an evolving microstructure. It was illustrated by the time evolution of cavities fields to highlight damage kinetics in gas-exposed rubbers upon decompression. More generally, this work provides methodological support for any physical process associated with significant morphological change. It can be applied to several types of phenomena occurring under deformation, e.g., damage (cavitation, cracking), kinematics of inclusions or phase transitions. Beyond classical statistical data about the microstructure (phase ratio, size and spatial distribution, etc.), covariograms provide information about REV and isotropy as a function of time. It is of special interest for micromechanical modeling, for example (i) to appreciate the relevance of deterministic modeling (deduced from ergodicity), (ii) to accurately depict the DREV in full-field simulations by the FEM method or (iii) to integrate accurate parameters in a schematic homogenization to take into account changes of microstructure morphology at the macroscopic scale.

Acknowledgements

This work pertains to the French Government program “Investissements d’avenir” (LABEX INTERACTIFS, reference ANR-11-LABX-0017-01).

References

[1] B.J. Briscoe, T. Savvas, C.T. Kelly, Explosive decompression failure of rubber: a review of the origins of pneumatic stress induced rupture in elastomer, Rubber Chem. Technol. 67 (5) (1994) 384–416.
[2] A.N. Gent, D.A. Tompkins, Nucleation and growth of gas bubbles in elastomers, J. Appl. Phys. 40 (1969) 2520–2525.
[3] J. Jaravel, S. Castagnet, J.-C. Grandidier, M. Gueguen, Real-time tracking and numerical simulation of cavity growth upon explosive decompression in hydrogen-saturated rubbers, Int. J. Solids Struct. 50 (2013) 1314–1324.
[4] D. Jeulin, Random texture model for material structures, Stat. Comput. 5 (2000) 121–132.
[5] D. Jeulin, Morphology and effective properties of multi-scale random sets, C. R. Mecanique 340 (5) (2012) 219–229.
[6] T. Kanit, S. Forest, I. Galliet, V. Mounoury, D. Jeulin, Determination of the size of the representative volume element for random composites: statistical and numerical approach, Int. J. Solids Struct. 40 (5) (2003) 3647–3679.
[7] G. Michaille, A. Nait Ali, S. Pagano, Two-dimensional deterministic model of a thin body with randomly distributed high-conductivity fibers, Appl. Math. Res. Express 2014 (2014) 122–156, http://dx.doi.org/10.1093/amrx/abt007, first published online December 16, 2013.
[8] C. Redon, L. Chermant, J.-L. Chermant, A mechanical damage model based on the measurement of microcrack orientation in concrete by Fourier transform, Acta Stereol. 16 (1997) 287–292.